AD731997

UNCLASSIFIED

Security Classification

DOCUMENT CONTROL DATA - R & D

(Security classification of title, body of abstract and indexing annotation must be entered when the overall report is classified)

1. ORIGINATING ACTIVITY (Corporate author)	2a. REPORT SECURITY CLASSIFICATION
Naval Ship Research and Development Center Bethesda, Md. 20034	UNCLASSIFIED
	2b. GROUP

3 REPORT TITLE

DESIGN AND PERFORMANCE OF BOW THRUSTERS

4. DESCRIPTIVE NOTES (Type of report and inclusive dates)

Final Report

5. AUTHOR(S) (First name, middle initial, last name)

John L. Beveridge

6. REPORT DATE	7a. TOTAL NO. OF PAGES	7b. NO. OF REFS
September 1971	45	18

8a. CONTRACT OR GRANT NO	9a. ORIGINATOR'S REPORT NUMBER(S)
SF35.421.006 b. PROJECT NO.	3611
c. Task 1713 d.	9b. OTHER REPORT NO(S) (Any other numbers that may be assigned this report)

10. DISTRIBUTION STATEMENT

APPROVED FOR PUBLIC RELEASE: DISTRIBUTION UNLIMITED

11. SUPPLEMENTARY NOTES	12. SPONSORING MILITARY ACTIVITY
	Naval Ship Systems Command Washington, D. C. 20360

13. ABSTRACT

This report concerns the hydrodynamic forces and moments produced by a bow thruster. Several broad problem areas are discussed and the extent of present-day knowledge indicated. These include general duct arrangement, duct shape, and impeller design.

A step-by-step design procedure is outlined that permits the selection of a practical bow thruster. This procedure is described for a minimum number of operational requirements; e.g., single bow thruster, a specified turning rate when the ship is dead in the water, and a duty cycle that requires thruster operation at ahead speed for control capability in canals, harbors and other restricted waterways.

DD FORM 1 NOV 65 1473 (PAGE 1)

S/N 0101-807-6801

UNCLASSIFIED

Security Classification

14 KEY WORDS	LINK A		LINK B		LINK C	
	ROLE	WT	ROLE	WT	ROLE	WT
Bow Thrusters						
Transverse Thrusters						
Maneuvering Devices, Auxiliary						

DEPARTMENT OF THE NAVY
NAVAL SHIP RESEARCH AND DEVELOPMENT CENTER
BETHESDA, MD. 20034

DESIGN AND PERFORMANCE OF BOW THRUSTERS

by

John L. Beveridge

September 1971 Report 3611

TABLE OF CONTENTS

	Page
ABSTRACT	1
ADMINISTRATIVE INFORMATION	1
INTRODUCTION	1
BACKGROUND	2
OPERATIONAL DUTY	4
PERFORMANCE FACTORS	5
STATIC MERIT COEFFICIENT	5
FORCE, MOMENT, AND VELOCITY	10
TURNING RATE	12
PRESENT KNOWLEDGE AND DESIGN CRITERIA	12
GENERAL ARRANGEMENT	13
DUCT INTERNAL SHAPE	15
DUCT OPENINGS	16
IMPELLER SELECTION	17
FLOW INTERACTION AT AHEAD SPEED	21
FREE RUNNING	23
THRUSTER SELECTION SUMMARY	23
REFERENCES	38
BIBLIOGRAPHY	39

LIST OF FIGURES

	Page
Figure 1 - Idealized Flow for Ducted and Open-Type Thrusters	27
Figure 2 - Typical Body Force and Body Moment Coefficient versus U_∞/U_j for a Bow Thruster	28
Figure 3 - Band of Rotation Rates versus Displacement with MPD at Zero Ship Speed (according to Reference 6)	29
Figure 4 - Pivot Point and Rotation Rate Constant for a Single Side Force Acting on a Ship (according to Reference 6)	30

Page

Figure 5 - Model Bow Thruster Installation 31

Figure 6 - Idealized Variation of ζ, C and T_p/T with Exit Area Ratio 32

Figure 7 - Criteria for Establishing Duct Lip Radius 32

Figure 8 - Relationship for Estimating the Resistance of Well-Faired Duct Openings 33

Figure 9 - Comparison of Merit Coefficient C as a Function of Thruster Pitch Ratio for Fixed and Trainable Maneuvering Propulsion Devices as Determined by Experiment 34

Figure 10 - K_Q versus K_T Obtained at Discrete Pitch Ratios for Adjustable Pitch Propellers (Noncavitating), V = 0 34

Figure 11 - K_T and K_Q versus Pitch Ratio for DSRV Bow Thruster with NSRDC Adjustable-Pitch Propeller 4160 35

Figure 12 - Ducted Thruster Cavitation Criteria Curves K_T and K_Q versus σ' (from Reference 9) 36

Figure 13 - Generalized Outflow Characteristics 37

Table 1 - Static Merit Coefficients for Circular Ducted Thrusters 11

NOTATION

A	Cross-sectional area of duct (nondiffusing)
A_I	Swept area of impeller
A_j	Cross-sectional area of thruster outflow
B	Maximum beam
C	Static merit coefficient
D	Duct diameter
g	Acceleration due to gravity
H	Ship draft or a net head, feet of water
K_F	Total side-force coefficient $T/\rho A U_j^2$
K_Q	Impeller torque coefficient $Q/\rho n^2 D^5$
K_T	Total side-force coefficient $T/\rho n^2 D^4$
L	Ship length or a characteristic length in general
ℓ	Duct length
M_o	Rotation rate constant, Figure 4
m	Fraction of length of thruster duct from bow, Figure 4
n	Impeller frequency of revolution, rps
P	Impeller pitch or a net pressure, $P_o - P_v$
P_o	Hydrostatic pressure (atmospheric + subm. to axis)
P_s	Power in consistent units
P_v	Vapor pressure of water
Q	Impeller torque
q_j	Jet dynamic pressure $\rho/2\ U_j^2$
R	Drag added by duct
SHP	Impeller shaft horsepower
T	Total thrust (side force) of impeller and surface forces
T_D	Duct surface force (thrust)
T_p	Impeller rotor thrust
U_j	Thrust momentum mean outflow velocity
U_∞, V	Undisturbed fluid velocity or ship speed

Ψ	Duct volume flow rate
x_T	Characteristic distance from duct axis to midships or c.g.
x_h	Impeller hub diameter as fraction of D
Δ	Displacement, tons
$\Delta C_p'$	Pressure coefficient $\Delta P/q_j$
ΔP	Difference between the pressure on the hull with thruster outflow and no outflow
ζ	Bendemann static thruster factor
ρ	Mass density of water
σ'	Cavitation index $(P_o - P_v)/\frac{1}{2}\rho D^2 n^2$
ϕ	Flow coefficient $\Psi/B^2 U_\infty$
ω_o	Turning rate, degrees per second

ABSTRACT

This report concerns the hydrodynamic forces and moments produced by a bow thruster. Several broad problem areas are discussed and the extent of present-day knowledge indicated. These include general duct arrangement, duct shape, and impeller design.

A step-by-step design procedure is outlined that permits the selection of a practical bow thruster. This procedure is described for a minimum number of operational requirements; e.g., single bow thruster, a specified turning rate when the ship is dead in the water, and a duty cycle that requires thruster operation at ahead speed for control capability in canals, harbors and other restricted waterways.

ADMINISTRATIVE INFORMATION

The work was authorized by the Naval Ship Systems Command and was funded under Subproject SF35.421.006, Task 1713.

INTRODUCTION

At the present time conventional circular transverse bow thrusters dominate the field of maneuvering propulsion devices (MPD) with respect to units installed. The literature on bow thrusters is replete with experimental and analytical data concerned with performance information and design criteria. Since many of these data can be generalized it is believed timely to review and tie together this information in one report. The performance of some bow thrusters could probably have been improved if certain information and knowledge had been available during their design. This is especially true with regard to duct size and the importance of the free-stream velocity in relation to the thruster outflow velocity in determining the total body force. Many types of thrusters have been installed and proposed for consideration and development. Included are: single and multiple units installed near the ships bow and/or stern, axial flow propellers, cycloidal propellers, ejector, ram, fixed pitch, controllable pitch and contrarotating.

In order to keep the present report of reasonable length, emphasis is placed on the hydrodynamically applied forces and moments due to a single bow thruster duct with a single fixed-pitch propeller (impeller). The combined action of multiple thruster units or coupling with rudder action is not considered. Such factors as wind, water current, ship motions,

etc. that require a knowledge of ship particulars and ship response are not within the scope of the present report. However, ship rotation rates that have been used satisfactorily in the past for bow thruster installations will be introduced. The report presents and discusses: performance factors or parameters which describe or aid in the evaluation of thruster performance, the extent of present knowledge and design criteria as related to configuration arrangement, duct geometry, propeller design, added resistance at ahead ship speed, and interaction of thruster jet flow with the mainstream. Particular details encompassed in this report are recommendations or criteria for the following design quantities: duct immersion, duct diameter, duct length, duct lip radius or shape, propeller hub-pod and fairwater effects, propeller blade shape and propeller pitch-diameter ratio.

A step-by-step design procedure which permits the selection of a practical bow thruster is outlined. This procedure is described for a minimum number of operational requirements; e.g., single bow thruster, a specified turning rate when the ship is dead in the water, and a duty cycle that requires thruster operation at ahead speed for control capability in canals, harbors, and other restricted waterways.

BACKGROUND

To assist in directing the designer to the more extensive areas of thruster work that have been published, the following background comments are made. It is suggested that the references cited be consulted for additional detail.

The work of Taniguchi[1] is very comprehensive and systematic. He conducted captive model tests as well as free-running model maneuvering tests. For static tests a standard test block which permitted variations in geometry of the duct configuration was utilized. Among the quantities investigated by systematic series tests were: *for the propeller* - blade outline, blade section, blade numbers, expanded area ratio, hub ratio, and pitch-diameter ratio; *for the duct* - duct wall inclination, grids, guide vanes, duct inner-wall shape, duct length, bottom immersion, duct opening

[1]References are listed on page 38.

lip radius, and duct opening fairing for three ship types (investigation of added resistance).

Chislett[2] has made measurements of body force and body turning moment on a captive tanker model. Special attention was given to explaining the effect of the ratio of model speed to thruster jet velocity. Implications to design and operation are rationalized based on the experimental results obtained at the ahead speed condition.

Taylor[3] has examined the effects of shroud (duct) lip radius, duct length, and duct diffusion on the performance of an air screw at the static condition.

Ridley[4] has presented some full-scale bow thruster data and the results of some American Shipbuilding Company series work with thruster entrance configuration. The possible beneficial effect of a truncated conic fairing with regard to added resistance was discussed.

Stuntz[5] has studied added resistance for several alternate fairings for tunnel openings and indicated how the flow patterns may be critically affected by the fairing detail. That combined fences and bars placed across the tunnel entrance (in the flow line) can effectively reduce resistance augmentation in some cases was demonstrated.

Hawkins[6] has made an extensive study of several types of MPD for the U. S. Maritime Administration. His work encompasses a spectrum of problems involved in the choice of an MPD and its design and performance. Maneuvering requirements, external forces, applied forces, and economic considerations are all discussed.

English[7] has shown that the ideal static merit coefficient is increased by the use of some jet diffusion. However, he points out that in practice the diffusion process is inefficient in a viscous flow for the typical short, wide-angled diffuser and consequently, little improvement in performance could be expected. An analytical study of duct inlet shape (constant velocity, elliptical, separation) was made. Practical considerations indicate that the duct-hull roundings required for good efficiency are not usually compatible with low added resistance.

Van Manen[8] has reported the results of comparative maneuvering tests for two tanker models. One model with a conventional propeller and rudder arrangement and one model with a Hogner afterbody, accelerating ducted propeller, and bow and stern thrusters (no rudder).

Pehrsson[9] has reported the results of a systematic series of tests in a water tunnel with a controllable pitch propeller. Bow thruster performance was related to the cavitation index σ'.

The Naval Ship Research and Development Center (NSRDC) has investigated by means of systematic experiments the effect of duct lip radius (at static and ahead operation), and propeller pitch ratio on bow thruster efficiency. A theoretical and experimental study of the interaction between an ambient flow and thruster inflow and outflow has also been made.[10]

Schwanecke[11] has reported a short chronology and summary of work on lateral thrusters.

OPERATIONAL DUTY

Two distinct maneuvering and control capabilities may be required of a bow thruster. On the one hand the critical maneuvering and control function may be when the ship is dead in the water or at extremely low headway. This type of duty cycle is exemplified by a variety of tenders or observation ships that must maintain station in the presence of wind, current, etc., or must execute changes in heading. Vessels which operate mainly in harbors and with frequent docking and undocking, such as ferries, also have this type of duty cycle. On the other hand the critical function for control may be for operation at a sustained ahead speed for long periods of time in restricted waterways such as coastal waters, canals and rivers. For this latter type of duty the design of a bow thruster must consider the interaction between the mainstream and the thruster jet flow which can compromise the design and performance of the bow thruster compared to that for an essentially static condition.

An obvious operational duty is that the thruster produce a body force and body moment to turn the ship to starboard or port. This duty cycle leads to a thruster design which incorporates symmetrical blade sections for the propeller and identically shaped duct entrance and exit openings. How this affects the thruster design will be discussed later.

Needless to say there are other operational duties and requirements (particularly for very specialized vessels including submersibles) that call for the use of multiple ducted thrusters or some other type of MPD. However, as stated previously these are not within the scope of this report.

PERFORMANCE FACTORS

STATIC MERIT COEFFICIENT

The useful work output given by the usual definition of propeller efficiency becomes zero at zero propeller advance. Since thrust is still produced, a measure of static (at rest) efficiency is needed to evaluate or compare thruster performance for this condition. Several forms of the "so-called" merit coefficient, figure of merit, static thrust efficiency, etc. have been widely used in both marine and aeronautical applications. In the latter case they have been used to characterize the performance of helicopter rotors and VTOL aircraft.

Most widely used are the static-merit coefficient

$$C = \frac{0.00182\ T^{3/2}}{SHP\ \sqrt{\rho \frac{\pi D^2}{4}}} = \frac{K_T^{3/2}}{\pi^{3/2}\ K_Q}$$

and the Bendemann static thrust factor

$$\zeta = \frac{T}{P_s^{2/3}\ D^{2/3}\ (\rho\ \pi/2)^{1/3}} = \frac{K_T}{K_Q^{2/3}} \cdot \frac{1}{\pi(2)^{1/3}}$$

where T is the total lateral thrust taken equal to the body reactive force,

SHP is the shaft horsepower,

P_s is shaft power in consistent units,

D is duct diameter,

ρ is mass density,

$K_T = \frac{T}{\rho n^2 D^4}$ is the usual propeller thrust coefficient,

$K_Q = \frac{Q}{\rho n^2 D^5}$ is the usual propeller torque coefficient, and

n is the propeller frequency of revolution.

These expressions are derived from momentum theory and can be shown to attain ideal (nonviscous) maximum values of $C_{max} = \sqrt{2}$ and $\zeta_{max} = 1.0$ for unshrouded propellers. For ducted propellers and with no duct diffusion $C_{max} = 2$

and $\zeta_{max} = \sqrt[3]{2}$. The following relation* exists between C and ζ:

$$\frac{C}{\zeta} = \sqrt[3]{\frac{2}{K_Q}} \sqrt{\frac{K_T}{\pi}}$$

or

$$C = \zeta^{3/2} \sqrt{2}$$

It is noted that with comparisons involving either C or ζ the higher the coefficient the more effective is the bow thruster; that is, more thrust per horsepower is developed. For equal total thrust comparisons,

$$T_1 = T_2 = \rho D_1^4 K_{T_1} n_1^2 = \rho D_2^4 K_{T_2} n_2^2$$

and for equal power comparisons

$$P_{s_1} = P_{s_2} = \rho D_1^5 K_{Q_1} n_1^3 = \rho D_2^5 K_{Q_2} n_2^3$$

which leads to

$$\frac{P_{s_1}}{P_{s_2}} = \frac{D_2}{D_1} \frac{K_{Q_1}}{K_{Q_2}} \left(\frac{K_{T_2}}{K_{T_1}} \right)^{3/2} \quad \text{for equal force}$$

and

$$\frac{T_1}{T_2} = \left(\frac{D_1}{D_2} \right)^{2/3} \frac{K_{T_1}}{K_{T_2}} \left(\frac{K_{Q_2}}{K_{Q_1}} \right)^{2/3} \quad \text{for equal power.}$$

---

*In the discussion (p. 370) accompanying Reference 5, an error of $\sqrt{2}$ appears in the maximum possible values given for C and its relation to ζ.

For the static case, Platt[12] has shown a relation between the thrust of a ducted and unducted propeller at equal power by the use of simple, nonviscous momentum theory. The same relation is derived here in a slightly different manner. The flow conditions are depicted schematically in Figure 1 where it is noted that ambient static pressure is assumed at the duct exit. The assumption seems reasonable from the standpoint that, in a real flow with considerable duct diffusion, the flow will separate before the exit and with little or no diffusion the approaching streamlines are essentially parallel, resulting in a jet-contraction coefficient of unity. Since the system is assumed to be conservative (no friction), all the power absorbed by the impeller is converted into kinetic energy in the final jet. Therefore, for the unducted case:

$$P_{UNDUCTED} = \frac{1}{2} m U_{j\infty}^2 = \frac{1}{2} \rho A_I \frac{U_{j\infty}}{2} (U_{j\infty})^2 = \frac{1}{4} \rho A_I U_{j\infty}^3$$

and for the ducted case,

$$P_{DUCTED} = \frac{1}{2} m U_j^2 = \frac{1}{2} \rho A_j U_j (U_j)^2 = \frac{1}{2} \rho A_j U_j^3$$

where P is fluid power,

m is mass flow per second,

ρ is mass density,

$U_{j\infty}$ is final slipstream velocity of the unducted propeller,

U_j is jet velocity of outflow from duct,

A_I is impeller disk area, and

A_j is area of duct outflow.

At the same power

$$P_{UNDUCTED} = P_{DUCTED} = \frac{1}{4} \rho A_I U_{j\infty}^3 = \frac{1}{2} \rho A_j U_j^3 \qquad (1)$$

From the change in momentum $T = \rho A_j U_j^2$ total thrust of ducted propeller, and $T_u = \frac{1}{2} \rho A_I U_{j\infty}^2$ unducted propeller thrust with the ratio

$$\frac{T}{T_u} = \frac{2A_j}{A_I} \left(\frac{U_j}{U_{j\infty}} \right)^2 \tag{2}$$

From Equation (1)

$$\left(\frac{U_j}{U_{j\infty}} \right)^3 = \frac{A_I}{2A_j}$$

or

$$\left(\frac{U_j}{U_{j\infty}} \right)^2 = \left(\frac{A_I}{2A_j} \right)^{2/3}$$

which when substituted in Equation (2) gives

$$\frac{T}{T_u} = \frac{2A_j}{A_I} \left(\frac{A_I}{2A_j} \right)^{2/3} = \left(\frac{2A_j}{A_I} \right)^{1/3} \tag{2a}$$

for equal power.

English has shown (Equation 6 of Reference 7) that, ideally, the Bendemann static thrust factor ζ is numerically equal to

$$\left(\frac{2A_j}{A_I} \right)^{1/3}$$

Thus from (2a)

$$\frac{T}{T_{UNDUCTED}} = \zeta = \left(\frac{2A_j}{A_I} \right)^{1/3} \tag{2b}$$

It follows from a previous definition that

$$C = 2\sqrt{A_j/A_I} \tag{2c}$$

Equations (2b) and (2c) are important and useful relations. For example, they indicate limiting ideal values* for ζ or C and show that for higher static thrust efficiency some duct diffusion is required. More will be said about this later.

Another important ducted propeller parameter is the ratio of impeller thrust to the total thrust T_p/T as a function of exit area ratio. The impeller thrust is determined by the pressure jump $(P_2 - P_1)$ which occurs across the disk area A_I; i.e.,

$$T_p = (P_2 - P_1)\, A_I$$

Writing the Bernoulli equation just behind and ahead of the impeller (Figure 1), we obtain

$$P_2 = P_o + \frac{1}{2}\rho\, U_j^2 - \frac{1}{2}\rho\, U_I^2$$

$$P_1 = P_o - \frac{1}{2}\rho\, U_I^2$$

or

$$P_2 - P_1 = \frac{1}{2}\rho\, U_j^2$$

whereupon

$$T_p = \frac{1}{2}\rho\, U_j^2\, A_I$$

---

*For a finite-bladed propeller the ratio of ducted propeller thrust to unducted propeller thrust at equal power has been found to be greater experimentally than is given by simple momentum theory.[3] This is probably because the bound circulation Γ goes to zero at the blade tip for the unducted propeller whereas the load is constant across the disk for the momentum model used.

and

$$\frac{T_p}{T} = \frac{1/2\ \rho\ U_j^2\ A_I}{\rho\ A_j\ U_j^2} = \frac{A_I}{2A_j} \tag{3}$$

Thus, for a straight-through circular duct (no diffusion), the total thrust is equally divided between the rotor and the duct. Further, it can be shown for this case that the duct surface force arises at the duct inlet and bears a resemblance to the suction force at the leading edge from thin airfoil theory.

Idealized curves of ζ, C, and T_p/T as a function of A_j/A_I are given in Figure 6. Because of its widespread use in this country and the usual problem of designing for a prescribed lateral force with minimum absorbed power, C will be used for performance evaluation in this report. Table 1 presents the static merit coefficient C for several bow thruster installations (no diffusion) reported in the literature.

FORCE, MOMENT, AND VELOCITY

In general, body total force and moment have been nondimensionalized in terms of impeller frequency of rotation or an average jet velocity U_j. The K_T and K_Q coefficients just defined in connection with the static merit coefficient are an example of the former case. It is also appropriate to use a nondimensional form of body coefficient which is independent of impeller characteristics. The jet velocity is convenient for this purpose as follows:

$$\text{Body force coefficient} \quad K_F = \frac{T}{\rho\ A\ U_j^2}$$

$$\text{Body moment coefficient} \quad N' = \frac{N}{\rho\ A\ U_j^2\ x_T}$$

where N is the body turning moment,

x_T is a characteristic lever arm (usually distance from duct axis to midships or c.g.),

TABLE 1

Static Merit Coefficients for Circular Ducted Thrusters

(No Diffusion, Model Data)

Bow Thruster Installation	Reference	Merit Coefficient C	Comment*
Shrouded airscrew in a plane wall	3	1.50	Best configuration, $x_h = 0.24$
DSRV		0.87	Stock design
DSRV		1.46	Final design, $x_h = 0.27$; Optimum P/D for given D
Markham	5	0.63	4×10^3 lb side force
Series	1	1.15	$A_e/A_o = 0.3$; $x_h = 0.4$; Highest merit coefficient among all variations
Series	1	1.18	$A_e/A_o = 0.52$; $x_h = 0.3$; Highest merit coefficient among all variations
Series	9	0.55 to 0.78	Propeller 317-B for $\sigma' = 3.0$ and P/D = 0.4 to 0.9
LST		0.82	800-hp unit; Blunt-ended hub-pod assembly (no fairwater)
LST		0.65	500-hp unit; Blunt-ended hub-pod assembly (no fairwater)

*C_{max} = 2.0 for a nondiffusing idealized thruster.

A is the duct cross-sectional area, and

$U_j = \sqrt{T/\rho A}$ is the momentum mean jet velocity based on static thrust.

Velocity U_j can also be calculated from a pitot survey made radially across the duct. A value near unity is obtained for K_F and N' at zero ahead speed, thus providing a fractional (percent) scale for the influence of ahead speed. A commonly used velocity ratio is U_∞/U_j. This form of the parameter is preferred to the inverse ratio which becomes infinite at zero ship speed. Figure 2 is a typical plot of these coefficients.

TURNING RATE

A design thrust for a bow thruster can be obtained if the ship response to the side force is specified. The turning rate ω_o (degrees/sec) when the ship is dead in the water is one performance criterion. The steady rotation of a ship not underway is basically a drag problem. By representing the ship as a flat plate with underwater dimensions of L and H, Hawkins[6] calculated ω_o for comparison with observed (measured) values of ω_o for a number of ships. The agreement in results was very close in most cases. Figure 3 presents Hawkins curves of measured turning rates as a function of displacement. The band given by these curves represents turning rates which have been considered satisfactory in past bow thruster installations. Figure 4 is a graph of the rotation rate constant M_o and nondimensional pivot point p as a function of nondimensional side force location. These are the Hawkins curves calculated for a single thruster acting on a flat plate.

PRESENT KNOWLEDGE AND DESIGN CRITERIA

Because of the complexity of the design problem of a bow thruster (which can exhibit strong interactions with the hull) some developmental experimentation may be necessary to approach or obtain an optimum configuration for a specific hull. However, certain basic flow phenomena, relationships, and performance characteristics are common to most bow thrusters, and, therefore, can be used in the design process to describe or determine their behavior. Thus, a great deal of the available experimental data can be exploited in a general manner as a guide in the design of bow thrusters. To this end such pertinent data and information are recounted.

GENERAL ARRANGEMENT

Location of the duct tunnel is hydrodynamically important but limited by practical considerations. Safety requirements dictate that it must be located behind the collision bulkhead. Space and other structural requirements must be satisfied. Strictly for the purpose of applying the thruster lateral force to obtain maximum body-turning moment, the duct should be located fairly far forward (probably not forward of station 0.10L). Hull curvature in the vicinity of the tunnel opening can significantly affect performance, particularly as related to added resistance (discussed later) at ahead ship speed and the fairing shape for the openings.

The need for an adequate duct length relative to the duct diameter further restricts the choice for duct location. Experiments by Taniguchi[1] show a rather broad flat optimum based on C between a length equal to 1D and 2D. A length equal to at least 2D is probably better because of the more rapid decrease in C that would be expected for very short ducts (i.e. $\ell < D$). Inasmuch as the duct diameter must usually be selected as a compromise only a tentative (initial) choice can be made. According to Taniguchi, bottom immersion should not be less than one duct diameter measured from duct axis to keel. Similarly, it seems reasonable that a minimum submergence of one diameter from the load waterline to the duct-axis should be maintained since wave action and ship motions would adversely affect bow thruster performance or added resistance. This might be a critical problem when the ship is running in ballast condition. In this regard, a possible problem for consideration is air drawing from the free surface by the ducted thruster unit. To the author's knowledge no detailed study of this problem leading to design criteria for propellers in relatively long tunnels at zero advance has been made. However, some bow thruster experiments for a LST at various drafts have been conducted at NSRDC. The results showed that with tunnel submergence (measured to axis) as low as 0.71D, no free-surface effect on side force or power was observed.

Shiba[13] has presented the results of an extensive study of air drawing of conventional unducted marine propellers. Of academic interest is the *necessary condition* postulated by Shiba as follows:

$$(P_a - P') b > 2S$$

where P_a is atmospheric pressure,

P' is the absolute pressure (including P_a) at a point on the body surface,

b is the width of the dead-water region, and

S is the surface tension between water and air.

It is perceived that the extent of the dead-water region due to laminar separation near the leading edge and the pressure decrement in that region are involved in the occurrence of air drawing. In the inequality, it is obvious that the atmospheric pressure drops out and that P' depends only on depth of submergence and a pressure coefficient of the body. Considering only the duct (but with impeller operating), a well-rounded duct inlet would not be likely to have a high suction peak or an extensive dead-water region. The experimental results presented by Shiba are for propellers at submergences $\leq 0.61D$.

An extrapolation of the Shiba data (for P/D = 1.0)* to zero J indicated that a submergence of at least $\approx 0.76D$ would be needed to avoid air sucking sufficient to affect propeller performance. Since the duct carries a substantial part of the total load of a bow thruster, it might be expected that less submergence is required to avoid detrimental air sucking in that case. That this is a reasonable assumption is substantiated by the previously mentioned LST tests.

Duct diameter is obviously a major factor in the installation cost and operating efficiency of a bow thruster. Large diameters may be more economical in horsepower but represent a heavier unit and a greater capital investment. For surface ship installations where cavitation might be a problem, it has been found that a $\sigma' < 3.5$ should not be used. This fact must be kept in mind for the final choice of diameter. Although no precise recommendation can be made here, a smaller diameter (higher rpm) thruster propeller may result in a less costly and more efficient prime mover.

To be discussed later is the problem of choosing a bow thruster diameter with regard to development of hull surface interaction forces when the ship duty cycle prescribes operation of the thruster with the ship underway.

---

*A near optimum value for ducted thrusters as will be seen later.

Another option which properly belongs in the realm of general arrangement is the choice of a fixed pitch or controllable pitch propeller. Extensive information and data are not available to permit a judicious evaluation of the relative merits of controllable versus fixed pitch propellers. Controllable pitch propellers permit thrust reversal where machinery rotation cannot be reversed. These propellers could lead to rather large hubs which decrease the overall performance (discussed later).

DUCT INTERNAL SHAPE

The constant area (nondiffusing) circular duct is apparently the favored form of tunnel for bow thrusters of the axial flow impeller type. English[7] has concluded that a bow thruster duct without diffusion is the most appropriate choice in practice. As shown previously the Bendemann factor

$$\zeta = \frac{K_T}{K_Q^{2/3}} \cdot \frac{1}{\pi(2)^{1/3}} = \left(2\frac{A_j}{A_I}\right)^{1/3}$$

is numerically equal to a function of the ratio of the outflow jet area A_j to the impeller swept area A_I. It can be seen from the above relation that for higher static thrust efficiency some diffusion is required. However, the typical bow thruster installation would lead to a rather inefficient short wide-angle diffuser. Additionally, English points out that the larger hull opening of the diffuser is undesirable from the standpoint of resistance, and that the relatively larger reduction in pressure on the suction side of the impeller would increase the danger of cavitation compared to a constant area duct.

Duct inner-wall shape was investigated by Taniguchi.[1] He used a series of three shapes that included (1) a standard parallel wall, (2) a concave wall (contracted entrance) to keep a constant flow area in the presence of the hub-pod assembly, and (3) a convex wall (expanded entrance) to evaluate static pressure recovery in the impeller outflow. Among these variations the standard constant area duct gave the highest static merit coefficient.

DUCT OPENINGS

Probably the most studied feature of bow thrusters has been the shaping of the duct openings. It is well known that for a jet flow the duct inlet should not have a sharp edge because infinite velocities are obtained in a frictionless flow and separation occurs at the edge in a viscous flow. A significant part of the total thrust produced by a ducted thruster is derived from the surface forces generated on the curved inlet and surrounding hull surface. With these factors in mind, it appears that some type of fairing radius or shape should be used. In contrast, the duct exit should have a sharp edge to assure stable outflow separation with minimum loss. Herein lies the great compromise because of the thrust (flow) reversal requirement of bow thrusters. A suitable fairing shape somewhere between a nice constant velocity inlet and a sharp edge outlet is desired. An almost uniform experimental result (see Figure 7) has been reported for the static mode of operation; for example,

Best r_{lip}/D	Reference
not less than ≈ 0.08	3 (for inlet only)
≈ 0.10	1
≈ 0.12	*

Tests at ahead speed with variable duct-lip radii conducted at NSRDC* showed little compromise choice between the best lip radius for the static and ahead modes of operation based on thruster performance. Stuntz[5] has recommended that a step be provided at the junction of the duct wall and the tangency line of the lip radii. The function of the step is to assure outflow separation with rounded duct openings. Since a step is undesirable on the entrance side there is probably a step size where the advantage at the outflow prevails over the disadvantage on the inflow. A step equal to 1/10 the maximum lip radius has been suggested,[5] and experimental results with this size step showed about a 3-percent increase in thrust producible per unit torque for a range of RPM.

*NSRDC Report not in the public domain.

If the duct openings are not fitted with doors, the effect of the duct openings on added resistance at ahead speed presents another consideration. Duct diameter and hull-duct opening fairing for high thruster efficiency are not completely compatible with low resistance. A method which is almost universally accepted as an effective solution to this extra drag problem is to form a conic fairing to remove the hard shoulder-like projection of the duct opening at the downstream edge. However, English[7] considers this procedure rather idealized in the sense that it is effective only for the case of pure forward motion. English has suggested that vanes placed vertically across the duct opening could be helpful in destroying the fore and aft momentum of the flow. Taniguchi[1] found a steady decrease in the merit coefficient C for horizontally placed grids (vanes) with increasing number of vanes. From no grids to five grids showed a 10-point drop in C. In Reference 1 the conclusion was reached that the added drag of duct openings is small for fine ships and considerable for full ships. Several ship types were tested (cable layer, liner, and super tanker) with variations in duct location on the hull and fairing shapes (including conical).

After testing and analyzing the resistance data of several bow thruster configurations, Stuntz[5] suggested the use in design of an average drag coefficient $C_D = R_{DUCT}/1/2\ \rho\ A\ V^2 = 0.07$ for carefully faired duct openings where ρ is the mass density of water,

A is the duct cross-sectional area,

V is the ship speed, and

R is drag added by the duct.

A dimensional relationship is provided in Figure 8 for convenience in estimating the resistance of duct openings with $C_D = 0.07$.

IMPELLER SELECTION

The importance of a hydrodynamically clean design for the internal arrangement of the supporting strut or struts and the impeller hub-pod-fairwater configuration cannot be overemphasized. It is desirable to keep the hub ratio x_h of the impeller (rotor) as small as possible and the entire configuration well streamlined. The following example shows what can be accomplished by proper attention to design detail. Some preliminary

static tests were made at NSRDC with a bow thruster unit which consisted of the lower half of a commercial outboard motor right-angle drive. A large hub ratio $x_h = 0.42$ was required with a very blunt (fineness ratio $L/D \approx 2.0$) hub-pod-fairwater configuration. Final static tests were made with the well designed right-angle drive shown in Figure 5. This arrangement had a modest hub ratio $x_h = 0.27$ and an overall fineness ratio $L/D \approx 8$. At the same impeller pitch ratio of 0.8, the static merit coefficient C was increased from an originally measured value of 0.87 to a value of 1.32 with the final design.

Several types of viscous and nonviscous losses[14] are associated with the blockage of a duct by the insertion of the necessary impeller driving arrangement. *Stream rotation* - The impeller torque developed in a frictionless flow leads to an induced tangential velocity. The average stream rotation and losses are dependent on the torque distribution and the hub size. *Diffusion* - A pod, impeller hub, and fairwater arrangement of finite length installed in a straight-through duct can be likened to the effect on efficiency of a typical wall diffusing section. Thus, losses are associated with diffuser efficiency as a function of the theoretical total-head rise in the rotor. *Separation* - Any condition, including too blunt a pod assembly, which leads to flow separation, may produce additional large losses.

Like open-water propeller systematic series, more can be learned concerning ducted propeller (bow thruster) performance by conducting experiments with a model or models, incorporating systematic variations in certain geometric parameters to determine the hydrodynamic characteristics of ducted propeller systems. This type of experimentation has been performed by several investigators,[1,9,15,16] and their test results provide the basis for most of the comments that follow. First, consider pitch ratio P/D. Experiments on shrouded propellers reported by Taniguchi,[1] Van Manen[15,16] and the author are in substantial agreement and confirm an optimum P/D near unity based on C for zero advance coefficient (static condition). A significant fact is that the merit coefficient attains a maximum value at $P/D \approx 1.0$ regardless of the tunnel type. That is to say, in each case the surface forces are dissimilar particularly for the Van Manen ducted propellers in an axial cylinder. The Van Manen Ka 4-55

data have been conveniently replotted for zero propeller advance coefficient to a base of pitch ratio in Figure 11-5 of Reference 6. Van Manen[16] has recommended the use of a constant face pitch (no radial variation) since his test results showed no "drawbacks with respect to efficiency and cavitation." Static efficiencies derived from all the aforementioned tests are summarized in Figure 9 together with other MPD types. In Figure 9, it is particularly noteworthy to see the penalty for operating a nondiffusing ducted thruster at a nonoptimum pitch ratio. Figures 10 and 11 show bow thruster coefficients K_T and K_Q obtained from experiments with adjustable pitch propellers.

Propeller blade outline and blade section shape have been studied for ducted propellers.[1] The consensus is that a blade outline with wide tips (Kaplan type) is desirable to better avoid cavitation.[17] Elliptical or some other symmetrical airfoil blade sections should be used to accommodate thrusting to port or starboard. With regard to blade number, the limited data available show an advantage of several points for the merit coefficient C of four blades over three blades.[1]

Pehrsson[9] has provided some cavitation data (see Figure 12) which can be used for guidance in the design of bow thrusters. His tests were conducted in the Kristinehamn cavitation tunnel. A duct with simulated ship plating was installed in the cavitation tunnel. A zero advance condition was maintained by bucking the bow thruster-induced flow by rotating the cavitation tunnel impeller pump in a reversed thrust direction. Cavitation observation and thruster force and duct force measurements (with 3-bladed and 4-bladed impellers having A_e/A_o = 0.43 to 0.50) indicated that the cavitation index

$$\sigma' = \frac{P_o - P_v}{1/2\ \rho\ D^2\ n^2}$$

should be >3.5 to avoid cavitation. Where doubt exists as to whether a "cavitation-free" design has been provided, a lifting-line design calculation should be performed.

For the static condition, the total delivered bow thruster force T consists of the impeller thrust T_p and the surface force T_D on the hull

inlet side. Earlier in this report it was shown that ideally with no duct diffusion, the total thrust is divided equally between the impeller and hull inlet. In a real flow with various losses the division of thrust is not equal. The location of a duct opening on a hull would result in a reduction in surface forces when compared to the case of a plane wall due to hull curvature and end effects. Values of $T_p/T \approx 0.8$ to 0.52 have been found in the literature. The lower value was measured for the case of a ducted airscrew in a plane wall.

A few words are needed in regard to performance estimates in connection with bow thruster design. In Table 1, an average value $\overline{C} = 0.94$ is obtained if the highest value of 1.50 (airscrew) and the lowest value of 0.55 (P/D = 0.4) are excluded. It seems likely that a C = 1.0 could easily be achieved in a well-designed thruster unit. Therefore, a conservative value of unity for the static merit coefficient C is recommended for performance estimates. An optimum P/D = 1.0 appears to be indicated by the available data. The total lateral thrust coefficients that have been reported in the literature for the best configurations are as follows:

P/D	K_T	Reference
1.0	0.51	*
1.0	0.40	1
1.0	0.45	9 (K_T is extrapolated from P/D = 0.9 to P/D = 1.0)

From these data an average value $\overline{K}_T = 0.45$ is suggested. How the average values for C and K_T are used in the thruster selection procedure is illustrated in the section "Thruster Selection Summary."

In conclusion it is emphasized that thruster impeller performance is negligibly affected by ahead speed as demonstrated by both comparative impeller thrust and torque measurements. Thus, impeller selection or design can be considered solely in terms of static performance.

*NSRDC Report not in the public domain.

FLOW INTERACTION AT AHEAD SPEED

It is well known that the interaction between bow thruster jet flow and the mainstream, at ahead speed, results in a loss of both body force and body moment, particularly, in a certain critical range of the velocity ratio $U_\infty/U_j \approx 0.2$ to 0.8.[2,10] In a theoretical and experimental study of this flow mechanism,[10] the author found only a small interaction due to duct inflow and confirmed the widely accepted hypothesis concerning the persistence of the duct outflow to large distances downstream accompanied by a major interaction effect.

A bow thruster is usually designed to produce a specified force at some ahead ship speed and on this basis the performance at ahead speed of different size bow thrusters should be compared at a jet velocity that varies inversely with duct diameter. One such comparison[10] showed that a smaller diameter duct produced less interaction (suction force) than a larger diameter duct at a higher ahead speed. Perhaps more important was the effectiveness of extending the duct beyond the hull (conceived as a retractable pipe extension) in the reduction of hull suction effect.

A phenomenological expression was derived in Reference 10 that collapsed all the hull pressure-defect data due to thruster outflow. A numerical evaluation of the necessary constants resulted in the following equation:

$$10^2 \, (\Delta C_p')\phi = (-9.052 \, D/L + 0.091) \sin [(-6830 \, D/L + 244.5)\phi] \qquad (4)^*$$

In Equation (4), the choice of hull length L to nondimensionalize duct diameter was made because (1) for a given thruster size, ship turning rate depends on hull length and (2) there is generally good agreement of flat-plate theory in this regard. Figure 13 compares the experimental results to those calculated according to Equation (4). The sine function form of Equation (4) was suggested by the shape of the curves of Figure 13. For no-duct outflow $(\Delta C_p')\phi$ is zero; at some higher value of ϕ, the coefficient $(\Delta C_p')\phi$ again becomes zero, corresponding to a relatively low value of

---

*Equation (2) of Reference 10.

velocity ratio U_∞/U_j where the thruster jet issues approximately perpendicular to the mainstream (static case). Within this interval, an equation of the form

$$(\Delta C_p')\phi = a \sin (x + B)$$

was assumed with $x = n\phi$, $a = f\ (D/L)$ amplitude, $n = g\ (D/L)$ period, and $B = 0$ phase. It is noted that the calculated curves should be faired with zero slope at the high-flow rate end.

Equation (4) is independent of scale, that is, the pressure $\Delta C_p'$ and flow coefficient ϕ were obtained from tests that were conducted at Reynolds numbers safely greater than the critical value for turbulent flow. Equation (4) may be used to estimate bow-thruster outflow interaction for a prototype based on comparative pressure defect. Flow coefficients are used that correspond either to prescribed values or to a desired range of velocity ratio U_∞/U_j and duct size. An elementary hull force, hull moment, and center of action of the force can also be derived by using the calculated pressure coefficient $\Delta C_p'$. The incremental surface force per unit width is

$$\frac{\Delta F_s}{\ell} = (\Delta P\ dS)\frac{dx}{dS} \tag{5}$$

where ℓ is in the circumferential direction and S is a length along the body profile. The nondimensional surface force, moment, and center of action are, respectively,

$$C_{F_s} = F_s/L\ell q_j = \int_{x=a}^{b} (\Delta C_p')\ dx \tag{6}$$

$$C_{M_s} = M_s/L^2\ell q_j = \int_{x=a}^{b} (\Delta C_p')\ x\ dx \text{ and} \tag{7}$$

$$\bar{x} = \bar{X}/L = C_{M_s}/C_{F_s} \tag{8}$$

Equations (6) and (7) give an index of the surface force and moment and do not consider jet diffusion over the hull surface. In many cases, this would not seriously impair the usefulness of the data. In the case of the comparison between the two ducts discussed earlier, the smaller duct had less pressure defect and this, coupled with the wider jet outflow of the larger duct, left no doubt that the smaller diameter duct would produce a lower interaction force.

Equation (4) can be used to estimate ΔP until more experimental data become available. The usual word of caution concerning the use of empirical data applies in this case: the accuracy for extrapolation purposes is unknown; therefore, the use of Equation (4) should be limited to interpolation or reasonable extrapolation.

FREE RUNNING

The results of captive model tests have formed the basis for comments and design criteria which have been presented so far. Very few experiments with free-running models have been reported. However, Taniguchi[1] has presented the results of extensive maneuvering tests. Of special interest to the designer is the Taniguchi inference (from recorded path loci of ship models) that in turning a ship smaller drift angles were observed by the use of bow thrusters than by the use of a rudder. Thus, speed reduction may be less in turning with a bow thruster. Norrby[18] has mentioned a few model tests which showed that the body turning moment from a bow thruster is increased at a drift angle, as in a turn, in comparison to the no drift angle case.

THRUSTER SELECTION SUMMARY

As an example consider a hypothetical ship with characteristic dimensions

$$\Delta = 3 \times 10^3 \text{ tons}$$
$$L = 275 \text{ ft}$$
$$B = 54 \text{ ft}$$
$$H = 17 \text{ ft}$$

Assume a duct centerline length of 12 ft is available at station 0.15L and a duty cycle that requires an effective turning moment at 3 knots of not less than approximately 80 percent of the static value.

Step 1. Initially, let the duct diameter D = 1/2 ℓ = 6.0 ft and the bottom immersion I = D. These are recommended values as discussed previously. Consider a D_{max} = 8.0 ft and a D_{min} = 4.0 ft. The situation is as shown below:

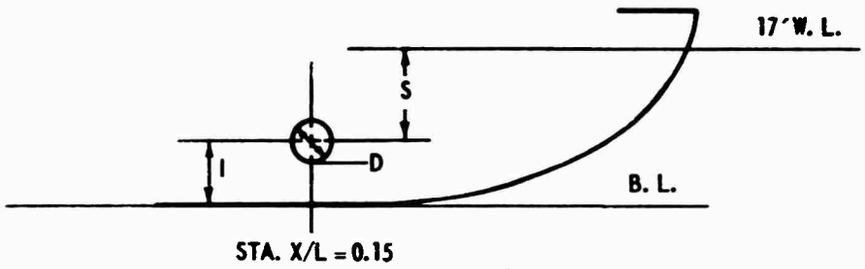

D in ft	I in ft	S in ft	ℓ/D
8	8	9	1.5
6	6	11	2.0
4	4	13	3.0

where it is seen that the submergence for D = 8.0 ft is still adequate.

Step 2. Pick an average turning rate for $\Delta = 3 \times 10^3$ from Figure 3 (say ω_o = 0.68 degrees/sec). The required thrust is

$$T = \frac{W_o^2 L^3 H}{M_o^2} = 17{,}380.\ \text{lb}$$

with M_o = 97 from Figure 4.

Step 3. With the specified static thrust, calculate the momentum mean jet velocity

$$U_j = \sqrt{T/\rho A} = 105.45/D \text{ and}$$

the velocity ratio U_∞/U_j at a speed of 3 knots (5.063 ft/sec) for each duct diameter

D in ft	U_j in ft/sec	U_∞/U_j
8	13.18	0.38
6	17.58	0.29
4	26.36	0.19

Step 4. Determine a tentative impeller rpm and σ' for the most likely diameter. In this case D = 4.0 ft based on the non-critical value $U_\infty/U_j = 0.19$ (see Figure 2). Impeller rate of revolution is determined from an inversion of the impeller thrust coefficient K_T. The average value $\overline{K}_T = 0.45$ which was recommended for an optimum impeller pitch ratio of 1.0 can be used. Thus

$$n = \sqrt{\frac{T}{\rho D^4 K_T}} = \left(\frac{17.38 \times 10^3}{1.9905(4)^4\ 0.45} \right)^{1/2} = 8.760 \text{ rps},$$

or 522.4 RPM, and

$$\sigma' = \frac{P}{1/2\rho D^2 n^2} = \frac{2978.}{0.9952 \times 16 \times 75.8} = 2.47$$

where 34.00 atmos.

13.00 submergence to ℄

47.00

-0.50 vapor pressure

46.50 Net head of water H, and

$P = \rho g H = 2978\ \text{lb/ft}^2$

Now, $\sigma' = 2.47$ is too low. σ' should be > 3.5.

Step 5. Repeat all calculations, for the specified thrust, using a new duct diameter; say D = 5.0 ft. The results are as follows:

$$I = 5.0 \text{ ft}$$

$$S = 12.0 \text{ ft}$$

$$L/D = 2.4$$

$$U_j = 21.09$$

$$U_\infty/U_j = 0.24$$

$$H = 45.5 \text{ ft of water}$$

$$n = 5.572 \text{ rps } (334.3 \text{ RPM})$$

$$\sigma' = 3.77$$

$$P/D = 1.0$$

It can be seen from the tabulation that all values are now acceptable, and D = 5.0 ft may be considered as the *final choice*. In some cases it may be necessary to use a nonoptimum P/D in order to obtain $\sigma' > 3.5$ with a consequent loss in efficiency.

Although a noncritical value of the velocity ratio U_∞/U_j is associated with the 5-ft duct diameter, a further check on duct outflow interaction at ahead ship speed may be obtained from Equation (4). Computations show that the argument 3.366 is not within the interval 0 to π (see Figure 13) for the specified relative duct size D/L = 0.0182. Therefore, no hull pressure defect (interaction) would be expected. However, the accuracy of the solution for $\Delta C_p'$ is questionable when the function $(\Delta C_p')\phi$ is near zero and some interaction* would be evident at the given velocity ratio $U_\infty/U_j = 0.24$, as shown by the moment curve for the typical surface ship in Figure 2b.

Step 6. Finally, estimate the power required from an inversion of the merit coefficient with C = 1.0 as recommended.

$$SHP = \frac{0.00182\ T^{3/2}}{C\ (\rho\ \pi D^2/4)^{1/2}} = 667$$

In closing the following remarks are made: It is important to realize when considering ahead speed operation, duct diameter need not be restrictive if controlled deflection of jet outflow is employed.[2,10] The

*Remember that a small change in pressure acting over a large area can produce an important force.

expected performance of the impeller is based on the desirable characteristics discussed previously; namely, Kaplan-type blade with symmetrical sections, expanded blade-area ratio of about 0.5, hub ratio $x_h \approx 0.3$ and three or four blades. It is emphasized that the design information and thruster selection method presented is a composite guide that should be reviewed as new data become available.

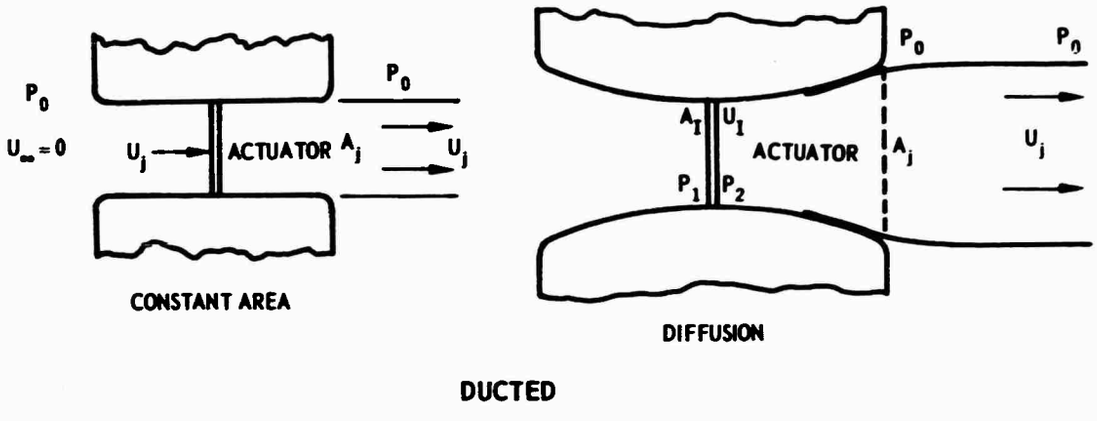

Figure 1 - Idealized Flow for Ducted and Open-Type Thrusters

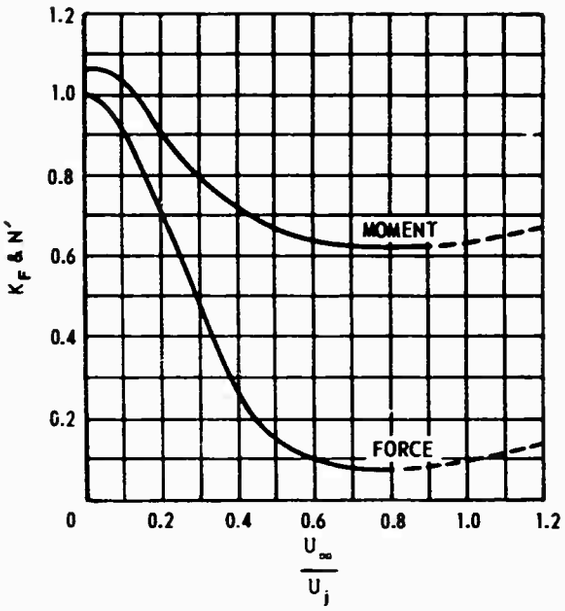

Figure 2a - Submersible

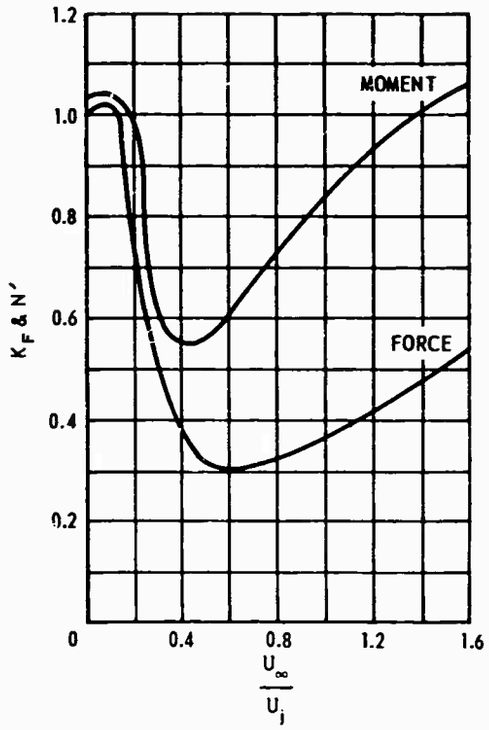

Figure 2b - Surface Ship
(According to Reference 2.)

Figure 2 - Typical Body Force and Body Moment Coefficient versus U_∞/U_j for a Bow Thruster

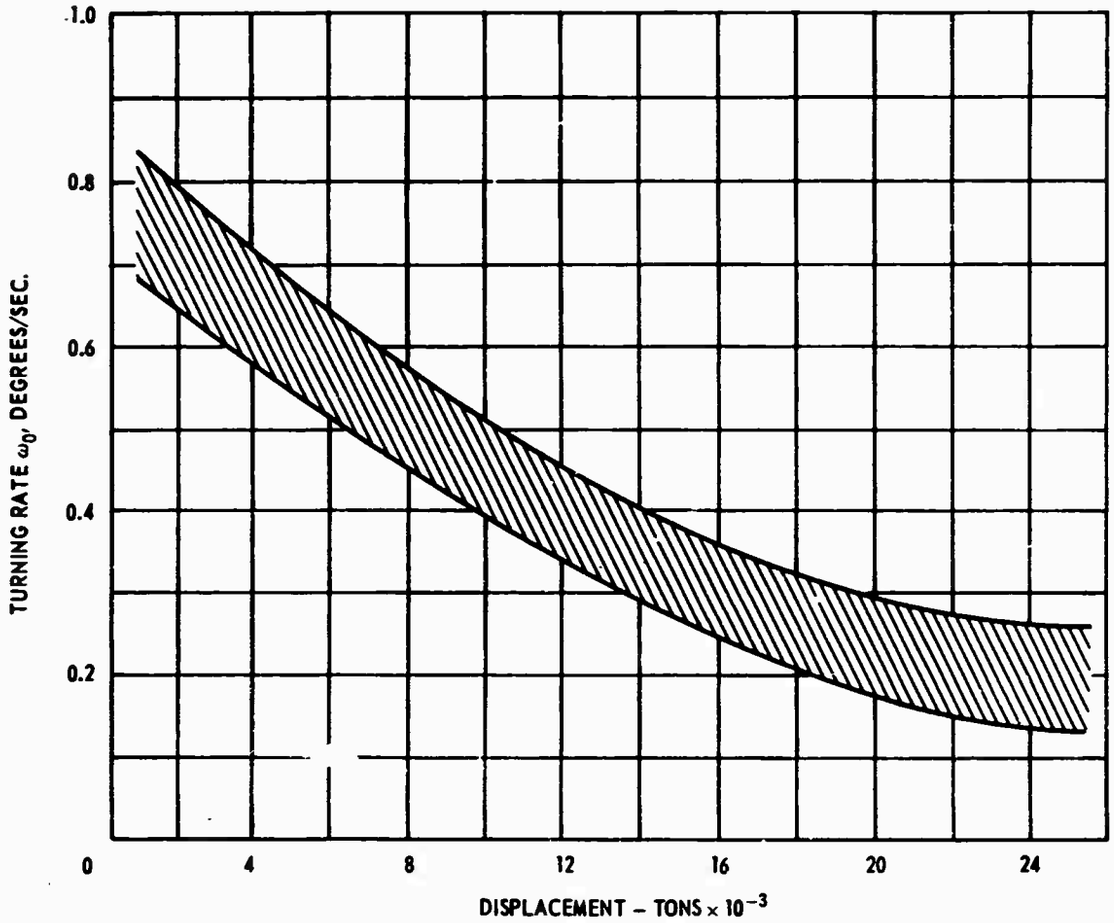

Figure 3 - Band of Rotation Rates versus Displacement with MPD at Zero Ship Speed (according to Reference 6)

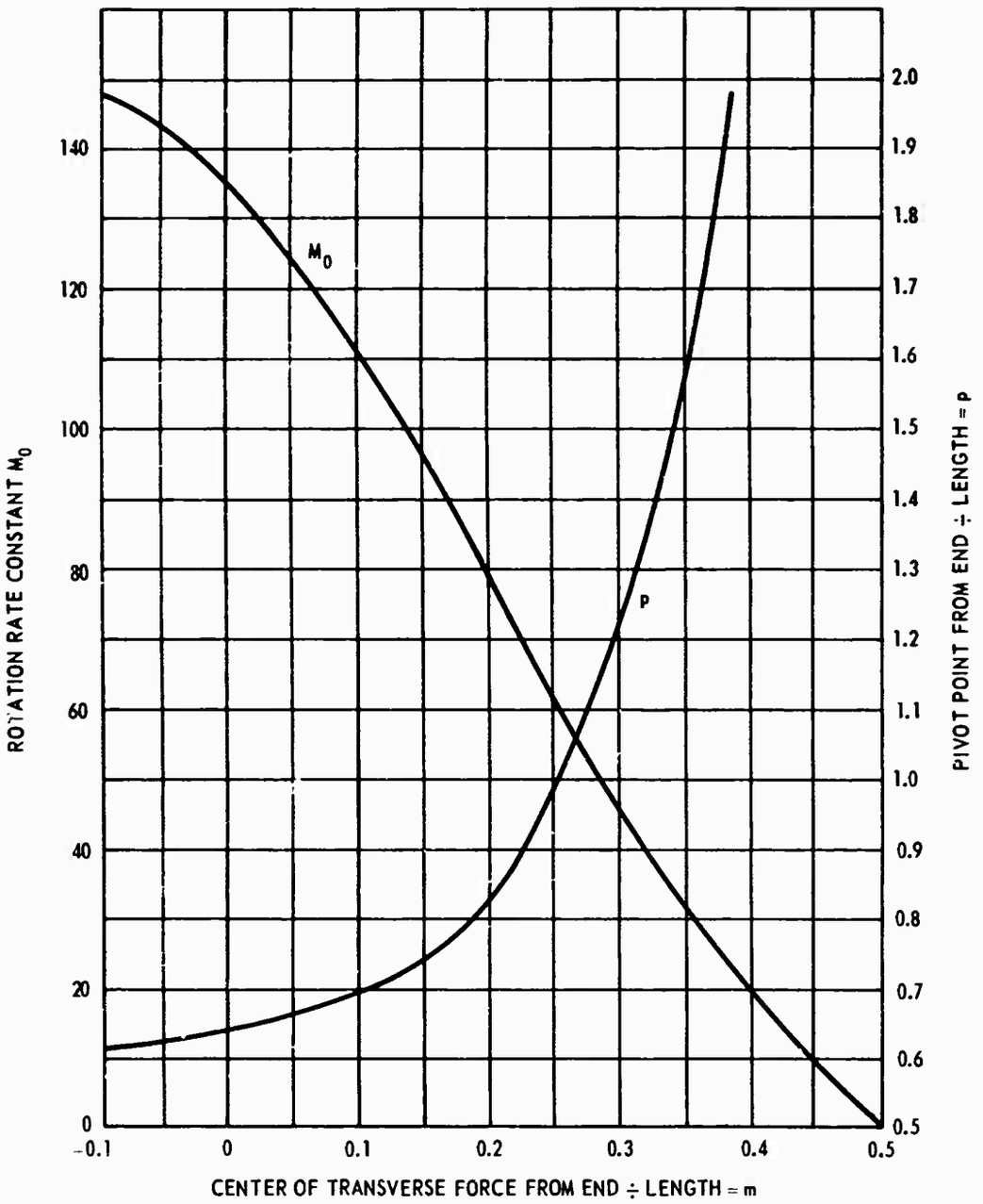

Figure 4 - Pivot Point and Rotation Rate Constant for a Single Side Force Acting on a Ship (according to Reference 6)

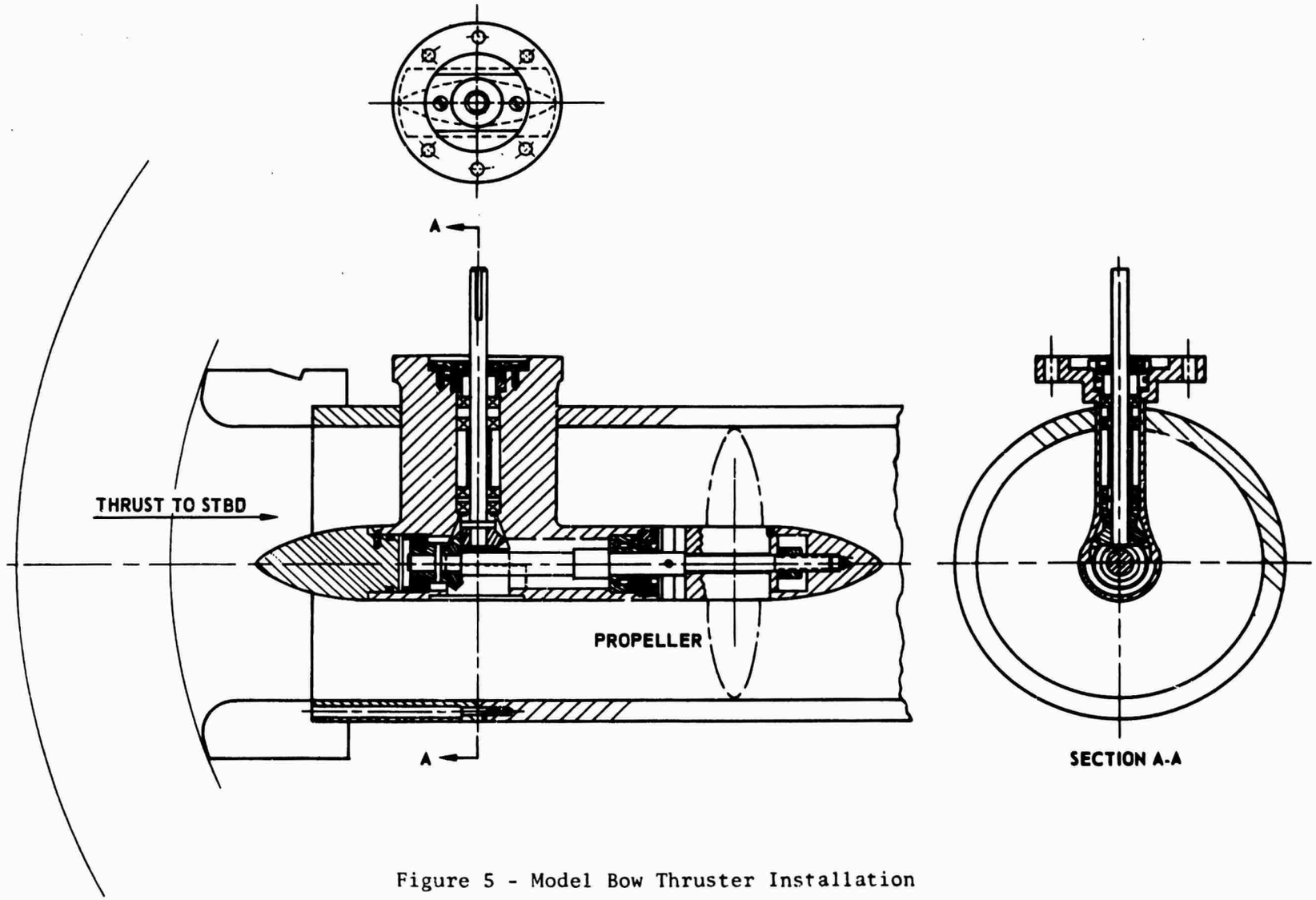

Figure 5 - Model Bow Thruster Installation

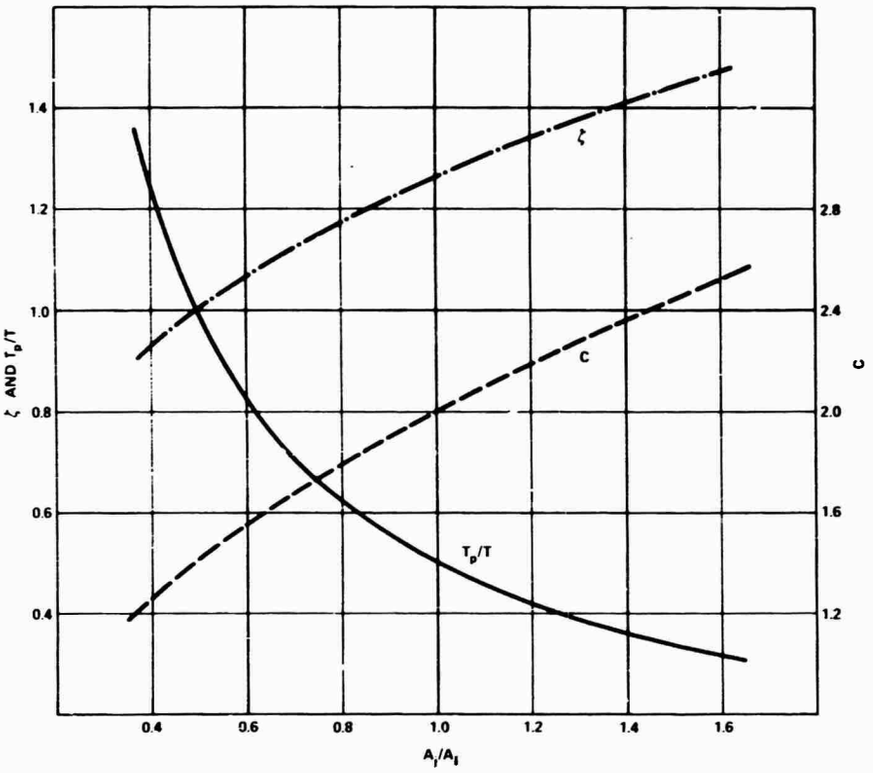

Figure 6 - Idealized Variation of ζ, C and T_p/T with Exit Area Ratio

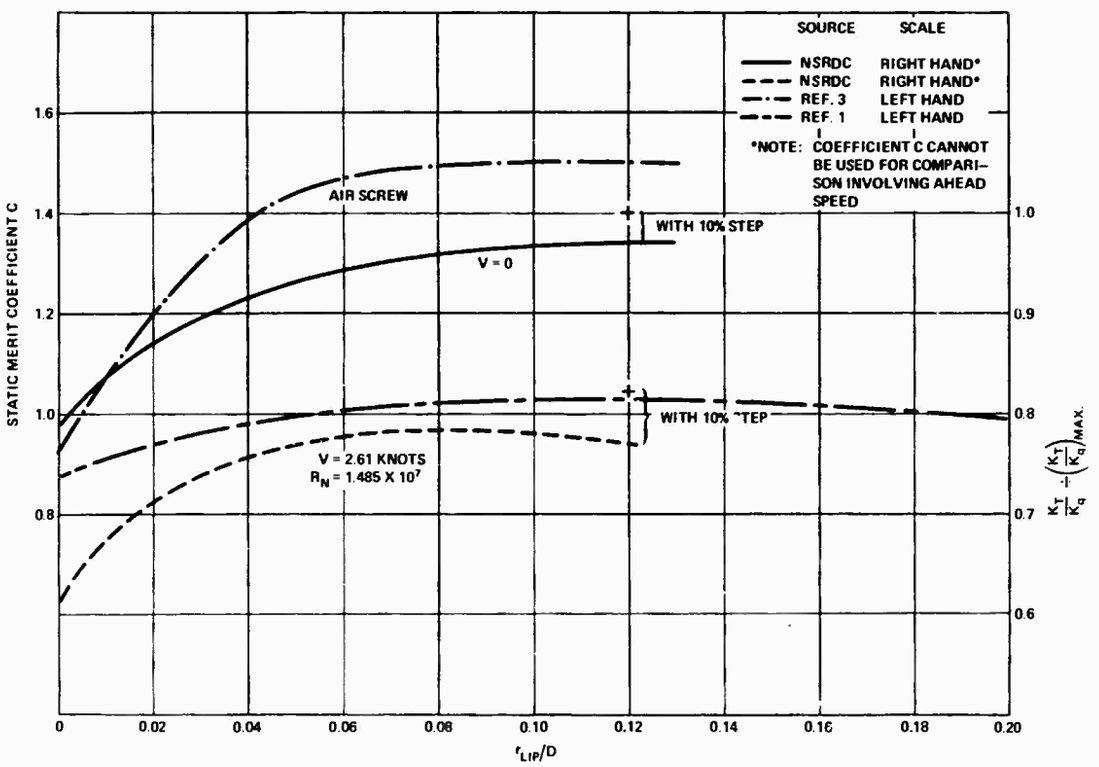

Figure 7 - Criteria for Establishing Duct Lip Radius

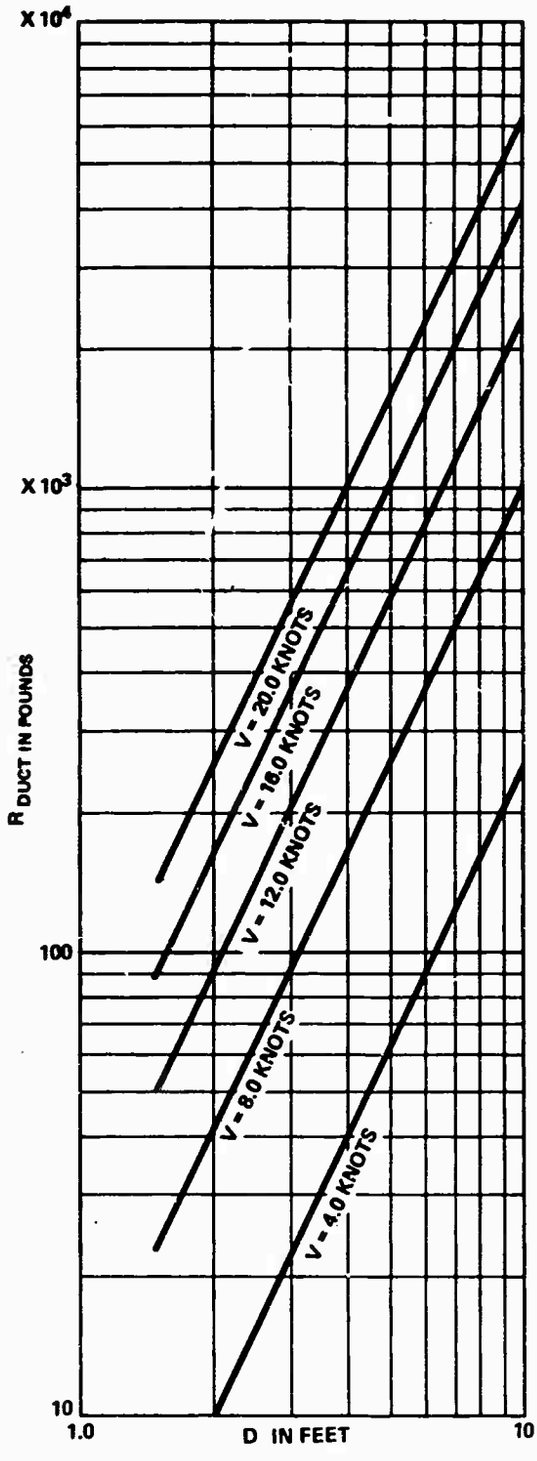

Figure 8 - Relationship for Estimating the Resistance of Well-Faired Duct Openings

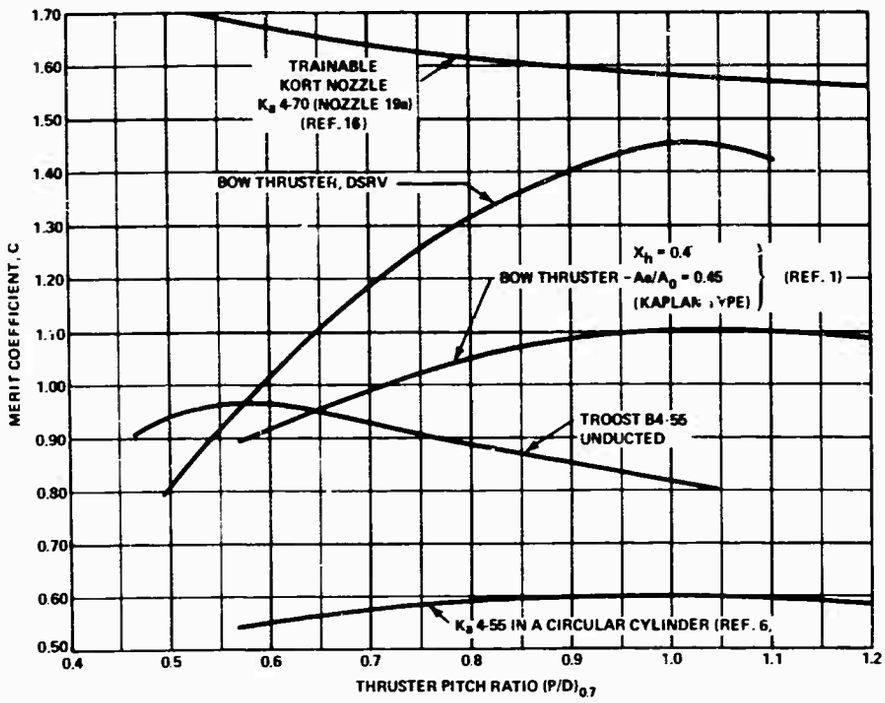

Figure 9 - Comparison of Merit Coefficient C as a Function of Thruster Pitch Ratio for Fixed and Trainable Maneuvering Propulsion Devices as Determined by Experiment

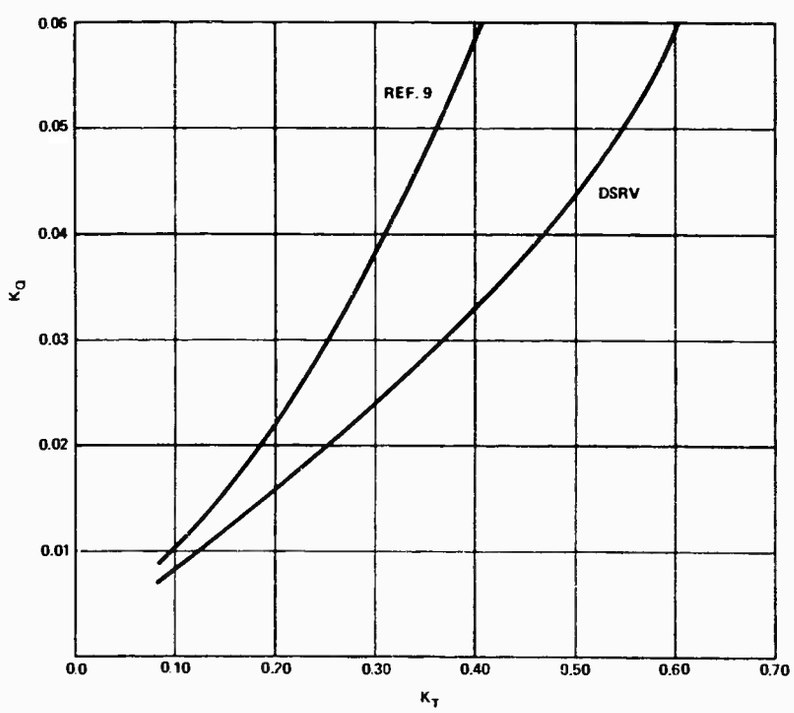

Figure 10 - K_Q versus K_T Obtained at Discrete Pitch Ratios for Adjustable Pitch Propellers (Noncavitating), V = 0

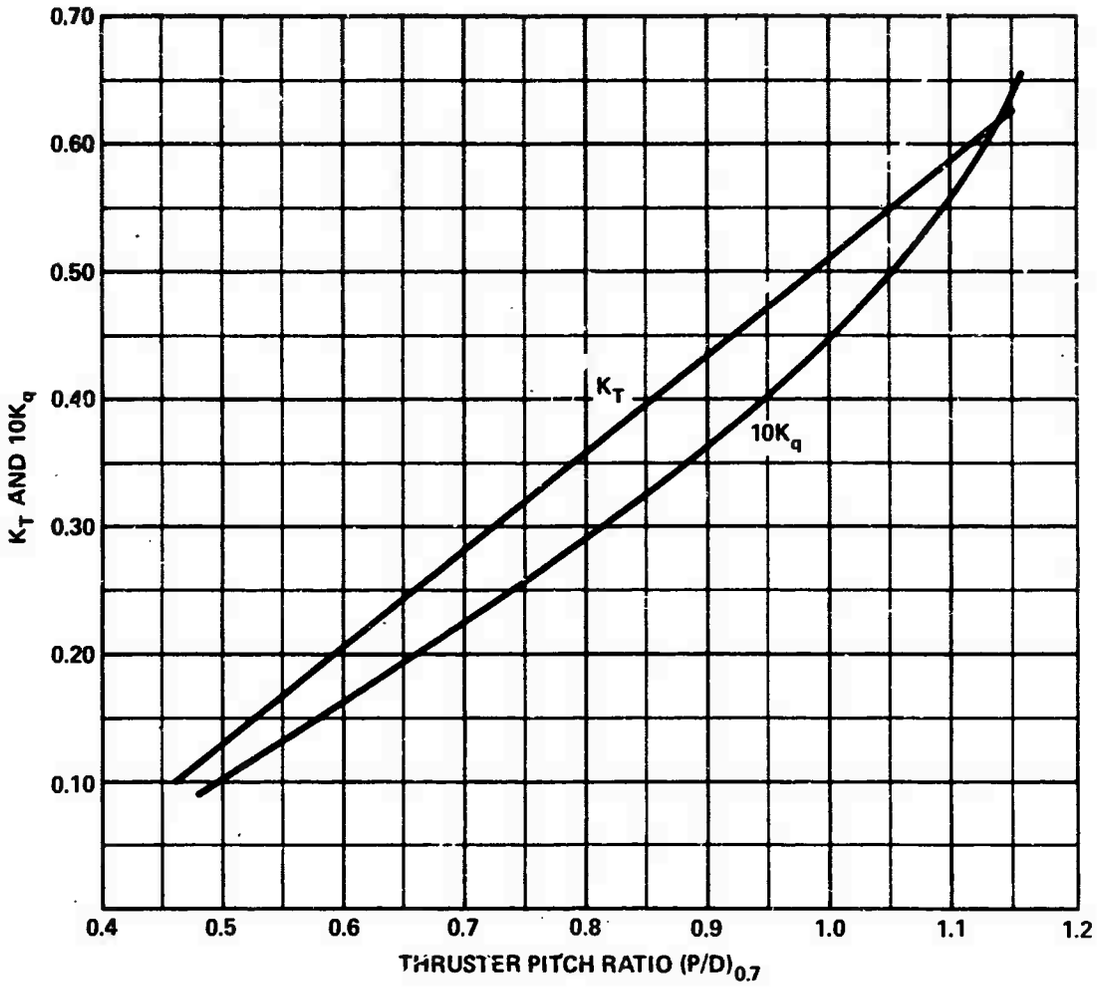

Figure 11 - K_T and K_Q versus Pitch Ratio for DSRV Bow Thruster with NSRDC Adjustable-Pitch Propeller 4160

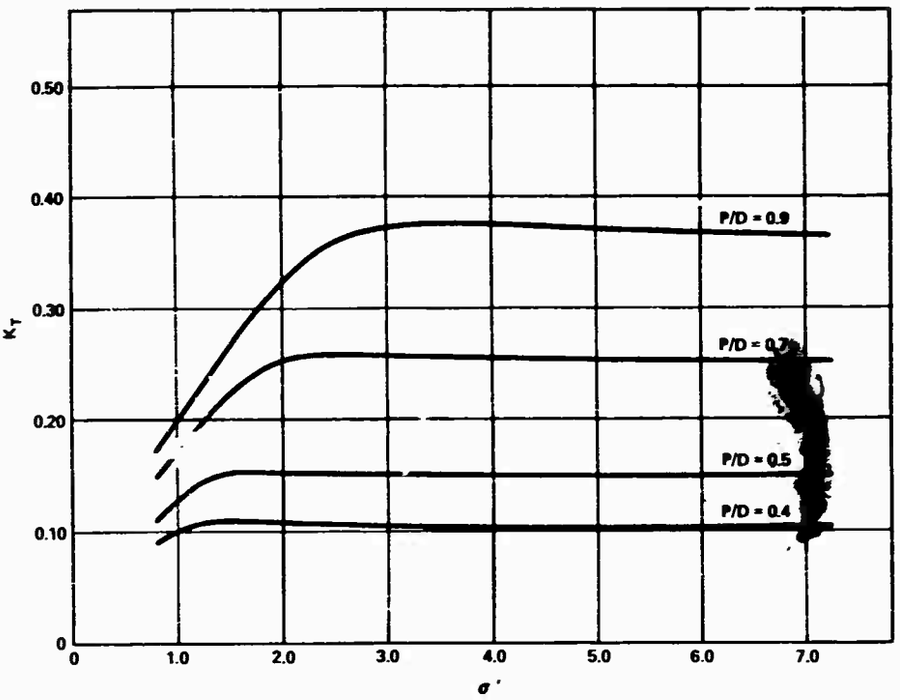

Figure 12a - Thrust Coefficient

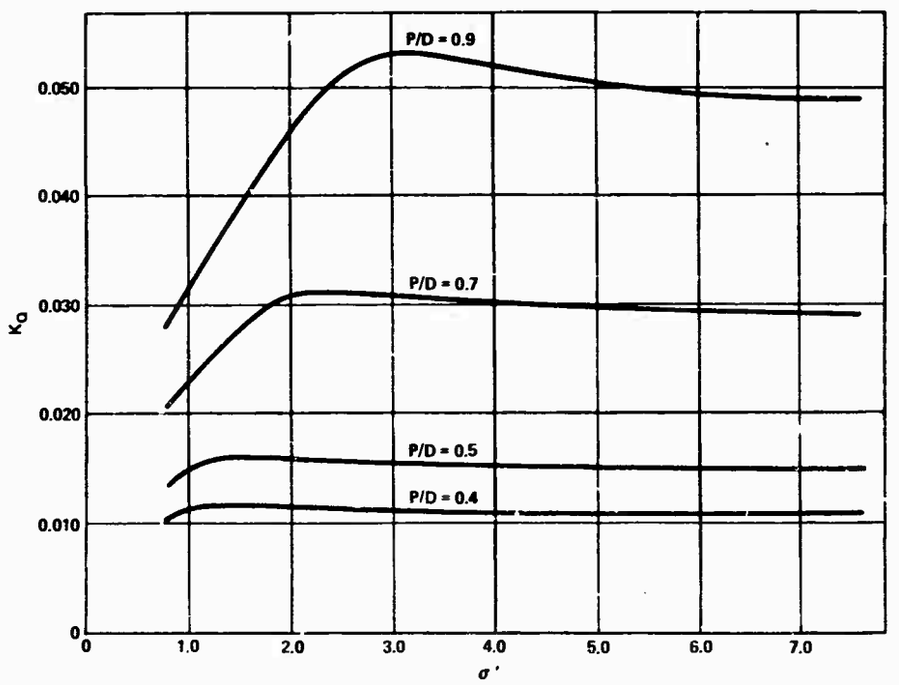

Figure 12b - Torque Coefficient

Figure 12 - Ducted Thruster Cavitation Criteria Curves K_T and K_Q versus σ' (from Reference 9)

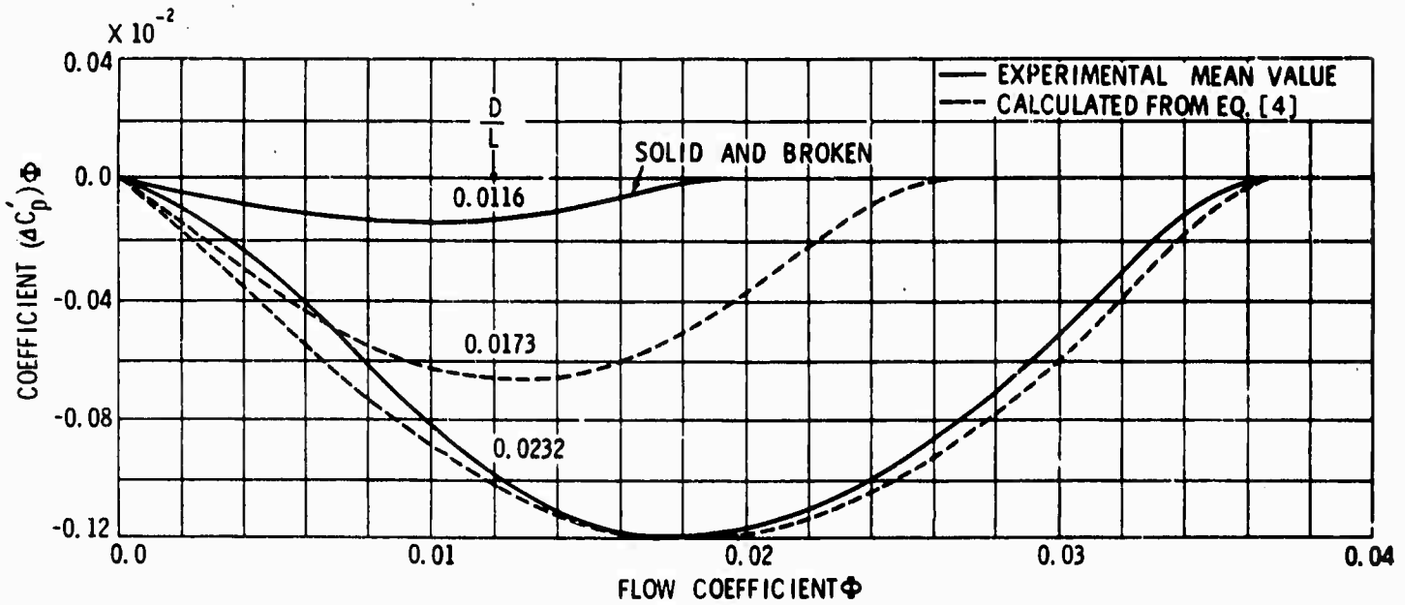

Figure 13 - Generalized Outflow Characteristics

REFERENCES

1. Taniguchi, K. et al., "Investigations into the Fundamental Characteristics and Operating Performances of Side Thruster," Mitsubishi Technical Bulletin 35 (May 1966).

2. Chislett, M. S. and Björheden, O., "Influence of Ship Speed on the Effectiveness of a Lateral-Thrust Unit," Hydro-og Aerodynamisk Laboratorium, Lyngby, Denmark, Report Hy-8 (Apr 1966).

3. Taylor, Robert T., "Experimental Investigation of the Effects of Some Design Variables on the Static Thrust Characteristics of a Small-Scale Shrouded Propeller Submerged in a Wing," Langley Aeronautical Laboratory TN 4126 (Jan 1958).

4. Ridley, Donald E., "Effect of Tunnel Entrance Configuration on Thruster Performance," SNAME Paper, San Diego Section (Sep 1967).

5. Stuntz, Jr., G. R. and Taylor, R. J., "Some Aspects of Bow-Thruster Design," Transactions Society of Naval Architects and Marine Engineers, Vol. 72 (1964).

6. Hawkins, Seth et al., "The Use of Maneuvering Propulsion Devices on Merchant Ships," Robert Taggart, Inc. Report RT-8518, Contract MA-3293 (Jan 1965).

7. English, J. W., "Further Considerations in the Design of Lateral Thrust Units," International Shipbuilding Progress, Vol. 13, No. 137 (Jan 1966).

8. Van Manen, J. D. et al., "Research on the Maneuverability and Propulsion of Very Large Tankers," Sixth Naval Hydrodynamics Symposium, Washington, D. C. (Sep-Oct 1966).

9. Pehrsson, Lennart, "Model Tests with Bow-Jet (Bow-Steering) Screw Propellers," First Symposium on Ship Maneuverability and David Taylor Model Basin Report 1461 (Oct 1960).

10. Beveridge, John L., "Bow-Thruster Jet Flow," J. of Ship Research, Vol. 15, No. 3 (Sep 1971).

11. Schwanecke, H., "Design of Lateral Thrusters (State of Art)," Twelfth International Towing Tank Conference Propeller Committee Report, Appendix VI (1969).

12. Platt, Robert J., Jr., "Static Tests of a Shrouded and an Unshrouded Propeller," NACA RM L7H25 (Feb 1948).

13. Shiba, H., "Air-Drawing of Marine Propellers," Transportation Technical Research Institute (JAPAN), Report 9 (Aug 1953).

14. Wallis, R. A., "Axial Flow Fans," New York and London, Academic Press (1961).

15. Van Manen, J. D., "Effect of Radial Load Distribution on the Performance of Shrouded Propellers," International Shipbuilding Progress, Vol. 9, No. 93 (May 1962).

16. Van Manen, J. D. and Oosterveld, M. W. C., "Analysis of Ducted-Propeller Design," Transactions SNAME, Vol. 74 (1966).

17. Van Manen, J. D. and Superina, A., "The Design of Screw Propellers in Nozzles," International Shipbuilding Progress, Vol. 6, No. 55 (Mar 1959).

18. Norrby, Ralph, "The Effectiveness of a Bow Thruster at Low and Medium Ship Speeds," International Shipbuilding Progress, Vol. 14, No. 156 (Aug 1967).

BIBLIOGRAPHY

Duport, J. and Renard J., "Panel Discussion 5 - Ducted Propellers," Seventh Hydrodynamics Symposium, Rome, Italy (Aug 1968).

Goodman, Theodore R and Chen, C. C., "Potential Flow Solution of Propeller Driven Jets Used for Submarine Depth Control," Oceanics, Inc. Report 64-18b (Sep 1965).

Jordinson, R., "Flow in a Jet Directed Normal to the Wind," Aeronautical Research Council, R & M 3074 (Oct 1956).

Keffer, J. F. and Baines, W. D., "The Round Turbulent Jet in a Crosswind," J. Fluid Mech., Vol. 15, Part 4 (Apr 1963).

Schaub, U. W. and Cockshutt, E. P., "Analytical and Experimental Studies of Normal Inlets, with Special Reference to Fan-in-Wing VTOL Powerplants," Proceedings of the Fourth Congress of the International Council of the Aeronautical Sciences, Palais de l'Unesco, Paris (Aug 1964).

"First Hydraulically Driven LIPS Transverse Propeller," Shipbuilding and Shipping Record (1 Aug 1963).